Rarefied Hypersonic Flow about Cones and Flat Plates by Monte Carlo Simulation

F. W. VOGENITZ* AND G. Y. TAKATA†
TRW Systems Group, Redondo Beach, Calif.

Rarefied flow of a monatomic gas about slender cones and flat plates has been studied by a numerical experiment at Mach numbers of approximately 10 and 25 for both hot and cold wall conditions. Cone semiapex angle ranged from 3° to 15° while the ratio of ambient mean free path to body length was varied from 0.01 to 3.0. Leading edge flow on sharp slender cones is found to differ substantially from that on flat plates in that surface fluxes for the former do not show the large overshoots above free molecule values which exist for the latter geometry. Monte Carlo predictions of flowfield properties and surface fluxes are shown to be consistent, in the main, with experimental data. The effect of intermolecular potential in near-free-molecule flow about cones was investigated.

Nomenclature

A = collision cross section
A_b = base area
A_s = surface area
D = base diameter
c = mean thermal speed
C_D = drag coefficient = drag/qA_b
K_D = Knudsen number = λ_∞/D
L = body length
L^* = L/λ_∞
M = Mach number
N = number flux
n = number density
p = pressure
Q = heat-transfer rate
Re_x = $\rho UX/\mu$
T = temperature
T^* = T/T_∞
T_0 = freestream total temperature
U_∞ = freestream velocity
X^*, Y^* = X/λ_∞, Y/λ_∞
γ = ratio of specific heats
λ = defined in Eq. (1)
ρ = mass density
ρ^* = ρ/ρ_∞
δ = cone semiapex angle
σ = hard sphere diameter
τ = shear stress
μ = coefficient of viscosity

Subscripts

$f.m.$ = free molecule value for diffuse reflection
w = wall value
inv = inviscid value
∞ = freestream conditions

Superscripts

$(-)$ = indicates normalization by the free molecule value; e.g., $\bar{p} = p/p_{f.m.}$

Received June 12, 1969; presented as Paper 69-651 at the AIAA Fluid and Plasma Dynamics Conference, San Francisco, Calif., June 16–18, 1969; revision received May 14, 1970. The authors wish to acknowledge the interest and support of the Advanced Research Projects Agency in this investigation. The work was administered through SAMSO Contract No. F04701-69-C-0019. The computer techniques used in this study were developed in collaboration with G. A. Bird, and the authors thank him for helpful advice regarding the simulation method.

* Member of the Technical Staff, Fluid Mechanics Laboratory. Member AIAA.
† Group Leader, Software and Computing Center.

I. Introduction

CONTINUUM equations retaining the framework of boundary-layer theory have been quite successful in treating the regions on a slender body upstream of the classical boundary-layer region, commonly called the viscous interaction regimes.[1] Experimental data are found to depart from the predictions of viscous interaction theory sooner or later as the leading edge of the body is approached,[2,3] and more general continuum equations have been used to attempt to describe the region still farther upstream where "merging," the disappearance of the inviscid region separating shock wave and boundary layer, is found to take place.[4,5] Somewhere upstream of the point of merging there lies a region often called the transitional regime in which the flow cannot properly be considered either collisionless or a continuum. This region extends upstream to include a few mean free paths forward of the leading edge, even for a sharp nosed body. Flows in this regime are usually characterized by a molecular velocity distribution which has departed significantly from the equilibrium Maxwellian distribution.

A Monte Carlo molecular simulation technique to describe this regime was originated some time ago by G. A. Bird.[6] A considerable virtue of this technique is that no arbitrary prescriptions are made about the form of the distribution of molecular velocities—this is derived completely from the calculation. Hence it can deal properly with highly nonequilibrium flows. Applications to a variety of problems have been described in Refs. 7–10. Hypersonic leading edge flow on flat plates was recently described with this technique.[11]

Recent measurements of surface pressure on slender bodies have shown that as the leading edge is approached (from downstream) the way in which pressure varies differs significantly between two-dimensional and axisymmetric geometries. For the flat plate, surface pressure rises from the inviscid value following the predictions of viscous interaction theory up to a value considerably above the free molecule (henceforth abbreviated f.m.) limit.[12] It is still above at a point only a few mean free paths (henceforth abbreviated m.f.p.'s) from the leading edge.[11] For a sharp slender cone the induced pressure rise above the inviscid value is much smaller and pressure is still below the f.m. limit at a point quite close (in m.f.p.'s) to the leading edge.[2,13] There is concern that many flat plate measurements have been affected by leading edge bluntness,[11] and the accuracy of all surface pressure measurements in rarefied flow is open to question; however, in spite of these uncertainties, there is no doubt that the differences commented upon previously are real.

In order to explore these differences, a Monte Carlo simulation study of transition flow about sharp slender cones was

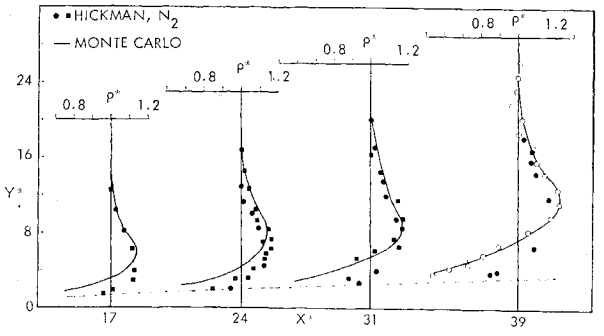

Fig. 1 Flowfield density profiles—5° cone, $M_\infty = 10.0$, $T_W = T_0$.

undertaken, designed to complement the study on flat plates presented in Ref. 11. A few additional solutions for flat plates were also obtained.

In contrast to the situation for flat plates, leading edge flow on cones, sufficiently close to the leading edge, has not been thoroughly explored experimentally, and there are only a few sets of data at widely differing conditions. Hickman[14] has made electron beam measurements of flowfield density for a 5° cone in nitrogen at $M_\infty = 9.4$, $T_w = T_0$. Kussoy and Horstman[2] have measured surface pressures in helium on a 5° cone with a hot wall at $M_\infty = 10.0$ and 29.2, while Waldron's[15] heat-transfer measurements on 5° and 10° cones with cold walls are at $M_\infty \cong 20.0$ in air.

The large number of parameters on which the flow depends has made it prohibitive for us to perform Monte Carlo, (henceforth abbreviated M.C.), calculations for the longer cones with a systematic variation of parameters. Rather we have concentrated on those cases enumerated for which experimental comparison of flowfield properties and surface fluxes is possible. The intent is both to demonstrate the accuracy of the simulation technique and to provide a more detailed description of the flow for these cases than can be obtained from the experimental data.

There is considerable interest in transitional cone drag, and it was possible to make calculations for short cones with a systematic variation of cone angle. These are compared with recent shock tunnel measurements of Geiger[16] and Kussoy and Horstman.[3] The effect of intermolecular potential on cone drag is also explored there. In general, calculations were made at Mach numbers of approximately 10 and 25 for both hot and cold wall conditions. The length Knudsen number, λ_∞/L, was varied from 0.01 to 3.0.

It is natural in studies of leading edge flow, using continuum equations, to view the flow looking upstream toward the leading edge with the reference properties those of the inviscid flow. We describe the flow in terms of departures from the free molecular limit since in so doing we retain some physical insight into the collisional processes by which the disturbance forms. Unfortunately, it is not clear what set of parameters forms a unified framework in which to view the flow from the leading edge through the viscous interaction regimes. Note that the differences between cones and flat plates cited earlier exist whether the reference pressure is the f.m. or inviscid value, since, for the flow conditions and cone angles studied here, the ratio of these quantities is approximately the same for both the cone and plate. For the cone there exists a moderate compression created by the geometry; i.e., $p_{f.m.}$ and p_{inv} are approximately an order of magnitude above p_∞, while for the plate they are of the same order. It unfortunately was not possible to include in this study the important case of the wedge, for which a strong compression above the freestream pressure level is created by the geometry.

II. The Simulation Technique

In this method the motion of a representative set of

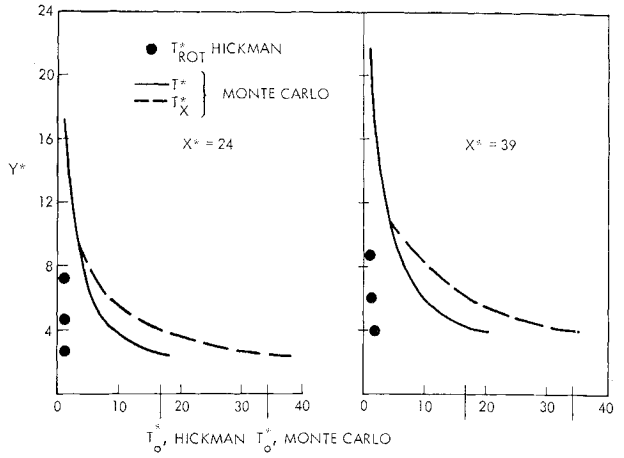

Fig. 2 Flowfield temperature profiles—5° cone, $M_\infty = 10.0$ $T_W = T_0$.

simulated molecules flowing past the body is followed exactly by digital computation while collisions in the gas are prescribed by statistical sampling. A detailed description of the simulation method has been given in Refs. 9–11. The principal approximations are as follows:

1) The movement of the molecules and the computation of collisions are uncoupled over an interval Δt which is small compared to the local mean free time $\bar{t}$.

2) To compute collisions in the gas the field is divided into a number of cells (typically several hundred) whose dimensions, Δx are small compared to gradients in the flow. The molecules in each cell are taken to represent the distribution function for that region, their locations within the cell are ignored, and collisions are prescribed by selecting pairs from each cell with the appropriate probabilities. Of course both of these introduce distorting influences in the calculation of the flow; e.g., there are some very fast moving molecules which have extremely small free times; conversely there are also some very slow moving ones which have very small free paths. The uncoupling interval and cell size must be set so as to distort the paths of only a negligible fraction of the molecules.

The effects of these approximations have been carefully investigated by making calculations over a range of values. The exact values used here varied with the flow conditions, but in general $\Delta t/\bar{t}_\infty \leq 1/M_\infty$ and, near a cold wall, $\Delta x/\lambda_\infty \approx 1/M_\infty$. The resulting distortions in these solutions are so small as to be undetectable in macroscopic flow properties.

The simulation procedure may be thought of as modeling the Boltzmann equation. The left hand side of that equation is satisfied, because we follow exactly the motion of each molecule. The statistical sampling procedure is constructed so as to produce the appropriate collision rate (consistent with the Boltzmann loss term) for all regions of velocity space; hence the collision integral on the right hand side of that equation is properly represented. It can be shown, by arguments too lengthy to reproduce here, that as the

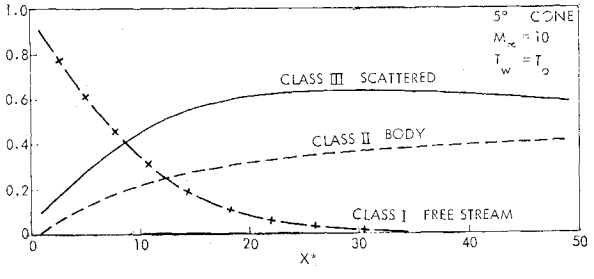

Fig. 3 Relative surface flux by molecular class.

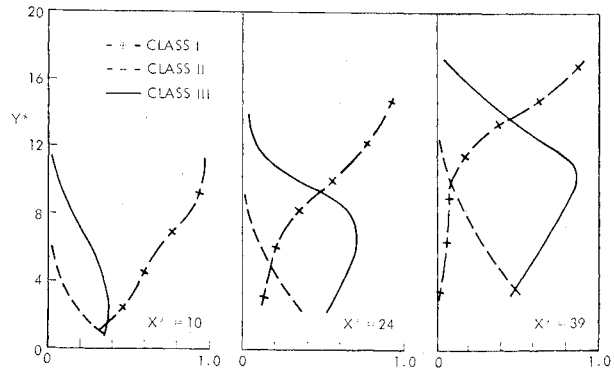

Fig. 4 Relative density profiles by molecular class—5° Cone, $M_\infty = 10.0$, $T_W = T_0$.

uncoupling interval and the cell size are made very small and the number of simulated molecules is made large the Monte Carlo solution tends to a solution of the Boltzmann equation, differing only by random statistical error.

III. Statistical Fluctuations

Statistical aspects of the simulation method have been discussed in Ref. 11. The results of the Monte Carlo calculations are shown here as lines which were faired by eye through sets of discrete points, with the extent of fluctuations indicated by a bar. Typical scatter is shown in Figs. 1 and 6

IV. Discussion of Results

Model Gas

Most of our calculations have been performed for a gas composed of hard sphere molecules which accommodate completely to solid surfaces and reflect diffusely, and we shall term this our "model gas." Unless otherwise noted, all results are for this model. We adopt this as a useful starting point while recognizing that the model may be inadequate to describe reality in some respects, especially near the body leading edge. A thorough study of these effects has not been made for this work, but where applicable, the results of such a study for flat plates in Ref. 11 will be noted. Calculations were also made in the near-free-molecule flow regime for molecules represented by point centers of inverse power repulsion, $F = Kr^{-\nu}$. Some of the effects of intermolecular potential will be discussed in the section on cone drag.

The effect of the trailing edge is found to be weaker on a cone at given flow conditions than for a flat plate. All flowfield and surface flux results presented are upstream of the region influenced by the trailing edge and hence are those for a semi-infinite body. All calculations discussed are for bodies with zero leading edge radius.

Length Scale

The Chapman-Enskog second approximation to the viscosity coefficient contains a length, viz,

$$\lambda = [32/5\pi(1 + \epsilon)]\mu/\rho c = 1/(2)^{1/2}An \qquad (1)$$

where $\epsilon = 0$ for Maxwell molecules (5th power), $\epsilon = 0.016$ for hard spheres; A = viscosity cross section[17] for power law molecules, $A = \pi\sigma^2$ for hard spheres. For hard spheres λ is Maxwell's mean free path for a gas at rest in equilibrium. Thus, whether we visualize the gas molecules as billiard balls or as point masses surrounded by force fields, a reference length and an effective size for the molecules deduced from freestream viscosity are nearly independent of the form of the potential. Most experimentalists determine a characteristic length for their results using freestream properties and Eq. (1). This approach has the advantage that the reference length is at least unambiguous, and freestream viscosity can be determined for most gases provided the temperature is not too low. However, in general λ_∞ is not a length of great usefulness in deducing how many collisions have occurred. It has long been recognized that a number of different mean free paths within the disturbance can be defined[18,19]; e.g., λ_{i-i} = mean free path of freestream molecule with respect to other freestream molecules, λ_{e-i} = mean free path of molecule emitted from body with respect to incident freestream molecules, λ_{i-e} = mean free path of incident freestream molecule with respect to emitted molecules from body, where these are all defined with respect to axes fixed in the body.

In hypersonic flows past a body with cold walls the mean free paths for different classes of encounter can differ considerably; e.g., $\lambda_{i-i}/\lambda_{e-i} \sim M_\infty^2$. It is sometimes claimed that it is more desirable to compare flows at a given ratio of some such length scale to the body characteristic length. We will discuss this approach in the section on cone drag. In our comparisons with experimental data we will scale all distances by λ_∞.

Comparison with Flowfield Measurements—5° Cone

Hickman's[14] electron beam measurements of flowfield density in nitrogen at $M_\infty = 9.4$, $T_w = T_0$ are compared with Monte Carlo profiles at a number of stations on the cone in Fig. 1, where the slow growth of a very weak disturbance can be seen. There is general agreement except near the wall where the computed density is somewhat lower than the data. We reserve comment on this difference until later.

There are a number of factors to be considered in this comparison. For the experiment the adiabatic wall condition results in $T_{\text{wall}}/T_\infty = 16.7$ whereas for the hard sphere gas $T_{\text{wall}}/T_\infty = 34.3$. Hence the wall is significantly colder in the nitrogen flow. Variations in wall temperature have been found to have a very weak effect on peak density in both measurements[20] and calculations[11] for flat plates. However, the thickness of the disturbance was found to de-

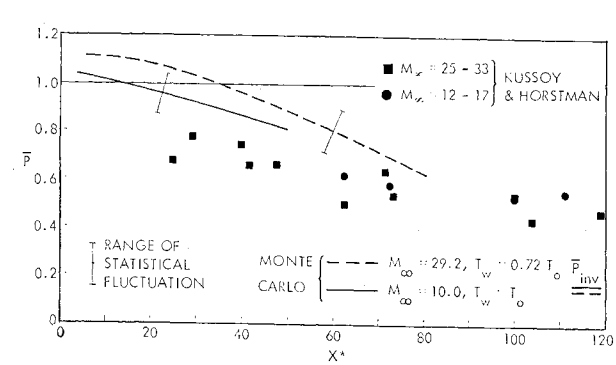

Fig. 5 Surface pressure—5° cone, hot wall.

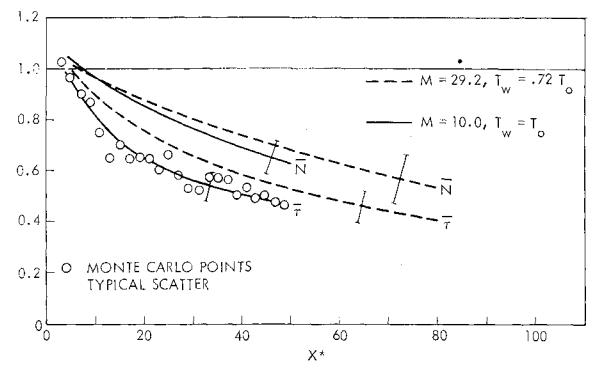

Fig. 6 Skin friction and number flux—5° cone, hot wall.

pend somewhat on the wall temperature and this is not evident in the comparison in Fig. 1.

One might also wonder about possible lack of accommodation in the nitrogen experiment. In Ref. 11 the effect of allowing 30% of the molecules to reflect specularly was found to become small at $x^* \approx 40$ for a cold flat plate at $M = 12.9$. However, evidence will be presented later to suggest that the point at which translational equilibrium is reached is located much farther downstream in x^* for a 5° cone than for a flat plate at these flow conditions. We conclude from this that the point at which the influence of the surface interaction law becomes weak is located farther downstream for the cone also. We will show later that the collisional activity in the gas is very weak, and it seems likely that at the stations shown, lack of accommodation would significantly affect the profile near the wall. An additional factor is that Hickman's freestream temperature was 10°K and our hard sphere model is too hard an interaction to represent a real gas at these low temperatures. Based upon the results of Ref. 11, it is estimated that a softer molecule, which more properly represents the cold nitrogen, would produce a slightly thicker and slightly weaker disturbance even at $x^* = 39$.

Finally, there is the effect of internal energy to be considered. Hickman's measurements of rotational temperature are shown in Fig. 2 where translational temperature T^* and a temperature computed from only the axial component of the molecular motion, T_x^*, are shown for the Monte Carlo calculation. The large difference between T^* and T_x^* at $x^* = 39$ shows that our model gas is still far from translational equilibrium there. Hickman's data indicate that the energy in the rotational mode is still essentially at the freestream level at $x^* = 39$ ($T_{rot}^* \approx 1.0$) and is still quite low ($T_{rot}^* \approx 3.0$) at $x^* = 91.5$. The nitrogen translational temperature was not measured; however, assuming the temperature jump at the wall to be the same fraction of T_0 as for the calculation would predict $T^* \approx 10$ in the nitrogen near the wall at $x^* = 39$. Evidently there is very large rotational lag in the nitrogen, and the flowfield properties should be close to those of a monatomic gas. The difference in wall temperature is the most likely explanation for the density difference near the wall between the M.C. result and the data. This seems to be indirect evidence of at least partial accommodation for kinetic energy.

The question of rotational lag should be studied directly by making calculations for molecules with internal degrees of freedom—such an extension of the technique is presently being carried out. However, lacking this, some insight can be gained by inspecting the collisional histories of the molecules by means of a scheme which is described next.

We divide the molecules into three distinct classes at any point in the flow by reference to their past histories; viz, class I—freestream molecules which have not been affected by the body, class II—molecules which at any time in their past history have struck and been reflected from the body,

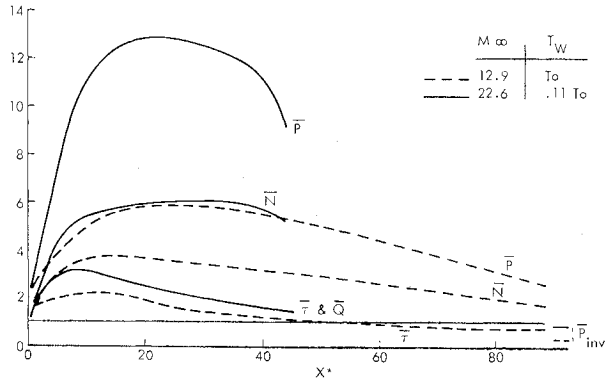

Fig. 7 Surface properties—flat plate.

Table 1 Average surface properties for short cones

8° Cone	$M = 24.0$		$T_w = 0.01\ T_0$	
λ_∞/L	$(\bar{P})_{av}$	$(\bar{Q})_{av}$	$(\bar{\tau})_{av}$	$(\bar{N})_{av}$
1.0	≈1.4	≈0.95	≈0.95	≈1.15

and class III—molecules which have been indirectly affected by the body by collisions in the gas. Class I molecules transfer to class II when they strike the body. Molecules once in class II remain there. Class I molecules transfer to class III when they collide with a member of either II or III. Class III molecules transfer to class II when they strike the body. G. A. Bird originated this classification scheme and has used it to display the simulated molecule motion on a cathode ray tube which is then photographed in triple exposure with the molecules of each class taking on a different color.[21]

The relative flux of each class of molecule to the 5° cone surface is shown in Fig. 3 where it can be seen that the flux of freestream molecules (class I) persists until $x^* \approx 35$. The mean free paths of incident molecules, λ_{i-s}, increases with distance from the cone surface because of the geometric decay ($\approx 1/r$) in the density of emitted flux. Incident molecules in the upper part of the shock layer then have quite long free paths. The fraction of flux due to class III molecules goes through a very flat maximum at $x^* \approx 25$ and then falls off very slowly. Profiles of the relative density of each class are shown in Fig. 4. The initially uniform profile of freestream molecules is gradually eaten away with distance downstream; however, at $x^* = 39$ a few freestream molecules still exist in the lower part of the disturbance. A boundary layer, represented by the class II profile, still occupies most of the layer at that station.

There is considerable evidence then, from which to construct a picture of a very slow relaxing shock layer with weak collisional activity which is still far from equilibrium at 39 m.f.p.'s from the leading edge. The measurements and the calculation are in fairly good agreement on these principal features.

Surface Properties—5° Cone

Computed surface pressure on a 5° cone at $M_\infty = 10$ and 29.2 is compared with the helium data of Kussoy and Horstman[2] in Fig. 5. The nose radius for the experimental model was $\approx \lambda_\infty$ and the data are far enough from the apex to be unaffected by this. It is seen that the surface pressure for our model gas is at a maximum only slightly above the free molecule value close to the apex of the cone and then falls off slowly, lying somewhat above the first experimental data points, but gradually approaching them. In a computer run of length sufficient for the sample size to be large enough on most of the cone surface, the sample is quite small very near the apex, and the properties there were not determined accurately for these conditions.

Shear stress and number flux for the 5° cone are shown in Fig. 6. Surface properties on a flat plate at $M_\infty = 12.9$, $T_w = T_0$ are shown in Fig. 7, where pressure, number flux and shear stress are seen to be substantially above f.m. values near the leading edge.

Surface Properties—8° Cone

In Fig. 8 surface properties for an 8° cone at $M_\infty = 24$, $T_w = 0.01\ T_0$ are shown. Pressure is seen to be slightly above the f.m. value with a broad peak near the apex.

There is uncertainty here also as to the values of $\bar{N}$, $\bar{Q}$ and τ very near the apex for the semi-infinite cone. The average properties on an 8° cone of length λ_∞ are shown in Table 1, where it can be seen that pressure and number flux are slightly above the f.m. values while skin friction and heat

Table 2 Departures from translation equilibrium

	$[(T_x - T)/T_0]$ $x^* = 39$	$x^* = 80$
Flat Plate $M = 12.9$, $T_w = T_0$	≈0.18	≈0.12
5° Cone $M = 10.0$. $T_w = T_0$	≈0.50	...
5° Cone $M = 29.2$, $T_w = 0.72\ T_0$	≈0.54	≈0.46
Flat Plate $M = 22.6$, $T_w = 0.11\ T_0$	≈0.21	...
8° Cone $M = 24.0$, $T_w = 0.01\ T_0$	≈0.44	≈0.38

transfer are slightly below. There is, of course, no reason to expect these to be identical with those for a semi-infinite body at $x^* \approx 1$, but it turns out they are in rough agreement with extrapolations of the curves shown in Fig. 8. Waldron's[15] heat transfer measurements in air on 5° and 10° cones at $M \approx 20$, $T_w/T_0 = 0.08$, are contained in the cross-hatched band lying below the Monte Carlo calculation.

The f.m. relationship between skin friction and heat transfer holds approximately from a point near the apex to $x^* \approx 80$—the faired M.C. curves differing by an amount too small to be shown on this scale.

Additional calculations have been made at hypersonic cold wall conditions for $\delta = 3°, 6°, 10°$ and 15°, and the trends for surface properties are roughly similar to the 8° cone results just presented.

Surface properties on a flat plate for hypersonic cold wall conditions are shown in Fig. 7 where a rapid rise to peak values substantially above the f.m. limit is evident for all properties. The free molecule relationship for skin friction and heat transfer is found to hold approximately for the plate also.

It is clear from the preceding comparisons that hypersonic leading edge flow on a slender cone differs substantially with respect to surface properties from that on a flat plate. This is perhaps not too surprising when one considers how the flow is established by collisions. For the plate, the disturbance is initiated by a weak thermal flux to the surface which when re-emitted induces a very large increase in the molecular flux to the surface by collisions with the freestream, sometimes called "cascading." For the cone angles studied here,

Table 3 Symbol identification Monte Carlo cone calculations

SYMBOL	CONE ANGLE δ	MACH. NO. M_∞	WALL TEMP. T_w/T_0	MOLECULAR MODEL
◁	3	24.0	0.01	H.S. = HARD SPHERES
○	6			H.S.
◇				12TH = 12TH POWER
△				5TH = MAXWELL MOLECULES
◑	6		0.13	H.S.
◑				12TH
◑				5TH
□	8		0.01	H.S.
▷		27.0	0.008	
▽	10	24.0	0.01	
	EXPERIMENTAL DATA			SOURCE
●	6	22.7 - 24.2	≈0.13	GEIGER, REF. 16
◆	15	22.7 - 24.2	≈0.13	GEIGER, REF. 16
◥	2.5	19.5 - 24.3	≈0.02	KUSSOY AND HORSTMAN, REF.3
■	5			
▼	10			

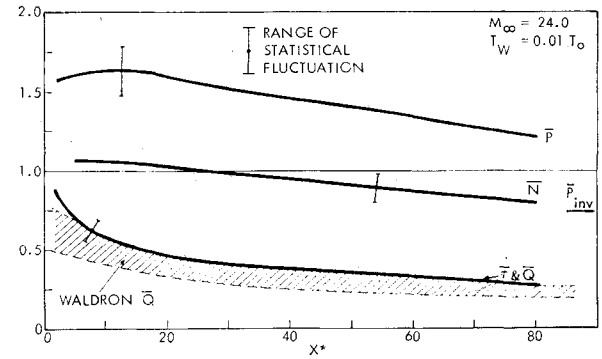

Fig. 8 Surface properties—8° cone.

the main contribution to the free molecule flux comes from direct impingement of the freestream on the surface. There is a geometric decay $\approx 1/r$ in the density of the emitted flux, and the solid angle subtended by the body for scattering back onto the surface is initially zero and grows slowly with distance from the apex. Hence, for the cone the initial induced departure from the free molecule flow is only a weak perturbation upon that flow.

Shock Layer Growth

The magnitude of the peak density in the disturbance would be expected to be a function of cone angle. We find that the disturbance on the 5° cone is considerably weaker than that on the plate at $M_\infty \approx 10$. McCroskey et al.,[12] have measured the peak density on a plate and a 10° cone at $M \approx 24$, $T_w \approx .15\ T_0$ and found that they are in agreement at $x^* \geq 125$. Our results for $\delta = 8°$ at $M = 24$ are roughly consistent with these findings in that for the x^* range covered $\rho_{peak}{}^*$ is not far below the plate value.

The rate at which the flow approaches translational equilibrium is also strongly affected by geometry. In Table 2 the peak departures from translational equilibrium are shown for cones and plates at various flow conditions. The values at x^* locations where comparison is possible are consistent with the picture derived from other properties; for slender cones the memory of the incident freestream is erased by collisions at a much lower rate than for a plate at the same flow conditions.

Sharp Cone Drag Coefficient

Computed drag coefficients for sharp slender cones with cold walls in our model gas at $M_\infty = 24.0$ are shown as open symbols in Fig. 9. Symbols are identified in Table 3. These were calculations for cones of finite length including a small portion of the wake. The sample size for most of these was ≈ 10,000, and the associated statistical uncertainty is ±4%. Solid symbols represent recent measurements in air and

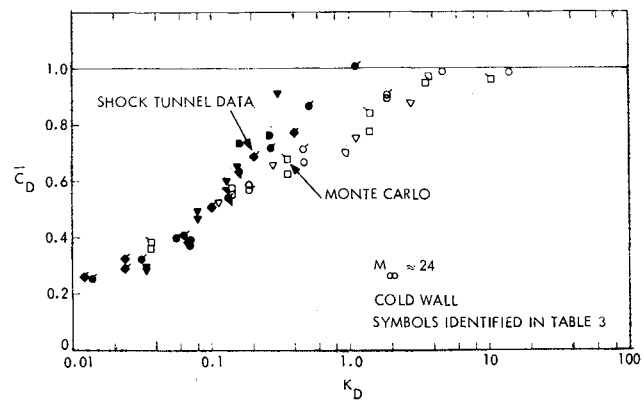

Fig. 9 Drag comparison for hard sphere molecules.

nitrogen obtained using free flight techniques in shock tunnels.[16,3] It is found that both calculations and measurements show a slight dependence on cone angle when plotted against λ_∞/L. When $K_D \equiv \lambda_\infty/D \approx \lambda_\infty/L \sin\delta$ is used as parameter, this effect is largely removed.‡

There has been speculation and controversy as to whether overshoots in cone drag above the free molecule value should be expected for a hard sphere gas on theoretical grounds. Laurmann's[22] first collision study predicts overshoots for cone angles less than about 9° while in the exact solution of the nonlinear Boltzmann equation obtained by Grad and Hu[23] the drag is always strictly less than the f.m. value. A Monte Carlo calculation for an 8° cone of length λ_∞ which was discussed earlier revealed that the average skin friction was slightly below the f.m. value while pressure and number flux were slightly above. Evidently the drag for $L \approx \lambda_\infty$ results from the delicate balance between a slightly increased flux with slightly reduced average axial momentum per particle. A very careful accounting of collisions in the gas must be made to compute the product correctly. Since the statistical uncertainty can never be removed completely, it would be difficult for a calculation of this kind to provide conclusive evidence as to whether or not the drag is strictly less than the f.m. limit. None of the present calculations, which extend up to $K_D = 4.75$ at $\delta = 3°$ and $K_D = 14.3$ at $\delta = 6°$, do exceed the f.m. value, and it seems likely that any overshoot contained in the Monte Carlo simulation for our model gas would be quite small. The shock tunnel data shown do not extend to values of K_D high enough to enable anything definite to be said regarding an overshoot. It can be seen that the data are somewhat higher than the hard sphere results above $K_D = 0.2$. These data, from Refs. 16 and 3, were obtained with freestream temperatures $\approx 18°K$ and $65°K$, respectively. For air there is a rapid change in the viscosity cross section between 18° and 250°K. Hence a moderately soft power law molecule might be more appropriate to approximate in some average sense the cross section variation in the test gas.

Calculations for $K_D \geq 0.2$ have been made for molecules represented by point centers of inverse power repulsion ($F = Kr^{-\nu}$) for $\nu = 12$ and 5. The range from hard spheres ($\nu = \infty$) to Maxwell molecules ($\nu = 5$) includes almost all gases of engineering interest,[24] with helium lying near the hard end of the scale and CO_2 near the soft end. The manner in which such molecules are simulated is discussed in Ref. 11. The surface interaction law used was again diffuse reflection and perfect accommodation. These results and the shock

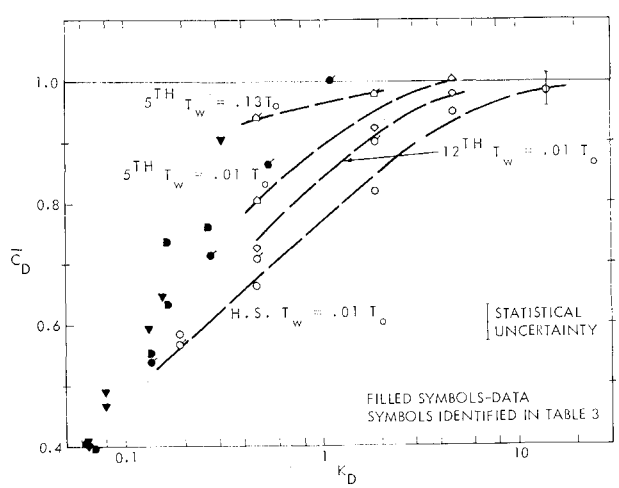

Fig. 10 Effect of molecular model on drag.

‡ The authors are indebted to J. A. Laurmann and R. E. Geiger for pointing out that λ_∞/D had some virtues in correlating experimental data.

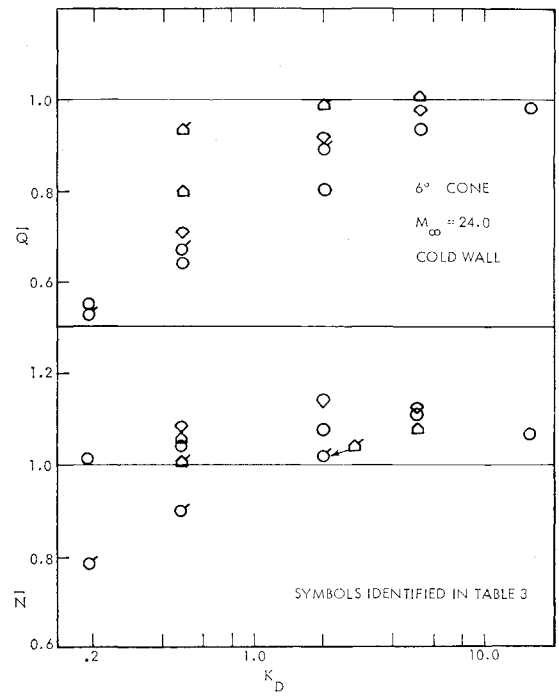

Fig. 11 Effect of molecular model on heat transfer and number flux.

tunnel data are shown on an expanded scale in Fig. 10, where curves have been faired through the points for clarity. It can be seen that when compared at a given value of λ_∞/D the drag increases as the molecule becomes softer (ν decreasing), and a modest increase in wall temperature has a much larger effect than for hard spheres, since the collision cross section is now velocity dependent. However, there is neither more nor less reason to expect an overshoot for the softer molecules than for hard spheres. For fixed λ_∞/D, as the molecule is made softer, the free paths in the disturbance become longer and collisions take place farther from the body. Thus there is less shielding of the body from the freestream, and the general falloff from the free molecule value is merely delayed to lower values of λ_∞/D. As the molecule is made softer, the M.C. drag curve does move toward better agreement with the shock tunnel data. It is not known which value of ν best approximates air at the experimental conditions; however, 5th power is certainly too soft for that. Hence at high K_D the Monte Carlo predictions are still below the data by a small amount for which we are unable to account.

In Fig. 11, heat transfer and number flux on a 6° cone at $T_w = 0.01\ T_0$ and $0.13\ T_0$ are presented for the various models. Not surprisingly, the variation of heat transfer ratio is similar to that for drag. Number flux exhibits an overshoot above the f.m. limit whose dependence upon wall temperature and model appears to be complex.

It is quite clear that the gross differences between results for the various molecular models in the near-free-molecule regime exist because the cross sections for all the models are matched in the free stream and there are large differences in cross section for the incident-emitted collisions occurring at relative velocity $\approx U_\infty$. The Monte Carlo drag curves for the various models and wall temperatures are roughly similar in shape, and they evidently could be at least brought closer together by modification of the abscissa length scale. It is known that the thickness, as well as the shape, of plane shock waves, when scaled by λ_∞, depends sensitively upon the intermolecular potential,[25,10] and it has been suggested that a more appropriate length scale can be defined which will remove or minimize this influence on thickness. (We are not aware of any claims that this procedure will correlate the

shape of the wave as well.) A number of candidate lengths have been proposed,[26-28] either determined within the disturbance or downstream of it. However, even for a plane shock wave in a given flow, these length scales can only be determined approximately and for a rarefied flow containing a cold body the uncertainty about the state of the gas in the disturbance is considerably larger. For example, using λ_{e-i} as a length scale provides too strong a correction and does not bring the $\bar{C}_D$ curves in Fig. 10 into coincidence. Careful study will be required to determine if anything useful can be accomplished along this line. Although there are not enough points to say definitely, it appears that the number flux curves in Fig. 11 may not have similar shapes, and modification of the horizontal scale alone will not correlate them, suggesting that the process of scattering back to the body from collisions in the gas may be essentially different for different potentials and wall temperatures.

V. Summary and Conclusions

1) Hypersonic leading edge flow on a sharp slender cone is found to differ substantially from that on a flat plate. For the flat plate the surface fluxes of momentum and energy rise sharply to peaks considerably above free molecule values a few m.f.p.'s downstream of the leading edge. For the cone these quantities are near their f.m. values at the leading edge and decrease with distance downstream.

2) The Monte Carlo predictions of flowfield properties and drag are shown to be consistent, in the main, with experimental data. Flows with different intermolecular potentials, when compared at the same freestream conditions, are found to differ significantly in the near-free-molecule regime. Some care is indicated in comparing measurements in this regime in different gases and/or at different temperature levels.

3) The Monte Carlo simulation technique has been demonstrated to be a powerful, useful method to describe the transition regime. The technique is believed to be in its infancy and large increases in scope and efficiency appear to be possible. Extensions to more general gases (internal degrees of freedom) and three-dimensional flows (simple shapes at angle of attack) are being carried out. The real utility of the method may lie in the feasibility to couple it with a continuum calculation: providing initial conditions (leading edge flow) or accepting initial conditions (expanding flows in nozzles and jets).

References

[1] Mirels, H. and Ellinwood, J., "Viscous Interaction Theory for Slender Axisymmetric Bodies in Hypersonic Flow," *AIAA Journal*, Vol. 6, No. 11, Nov. 1968, pp. 2061–2070.

[2] Kussoy, M. I. and Horstman, C. C., "An Experimental Study of Hypersonic Rarefied Flow over Sharp Cones," *Rarefied Gas Dynamics*, Supplement 5, Vol. I, Academic Press, New York, 1969, pp. 607–618.

[3] Kussoy, M. I. and Horstman, C. C., "Cone Drag in Rarefied Hypersonic Flow," *AIAA Journal*, Vol. 8, No. 2, Feb. 1970, pp. 315–320.

[4] Shorenstein, M. L. and Probstein, R. F., "The Hypersonic Leading Edge Problem," *AIAA Journal*, Vol. 6, No. 10, Oct. 1968, pp. 1898–1906.

[5] Cheng, H. K. et al., "On the Hypersonic Leading Edge Problem in the Merged Layer Regime," *Rarefied Gas Dynamics*, Supplement 5, Vol. I, Academic Press, New York, 1969, pp. 451–463.

[6] Bird, G. A., "Approach to Translational Equilibrium in a Rigid Sphere Gas," *The Physics of Fluids*, Vol. 6, 1963, pp. 1518–1519.

[7] Bird, G. A., "Aerodynamic Properties of Some Simple Bodies in the Hypersonic Transition Regime," *AIAA Journal*, Vol. 4, No. 1, Jan. 1966, pp. 55–60.

[8] Bird, G. A., "The Velocity Distribution Function Within a Shock Wave," *Journal of Fluid Mechanics*, Vol. 30, Pt. 3, Nov. 1967, pp. 479–489.

[9] Vogenitz, F. W. et al., "Theoretical and Experimental Study of Low Density Supersonic Flows About Several Simple Shapes," *AIAA Journal*, Vol. 6, No. 12, Dec. 1968, pp. 2388–2394.

[10] Bird, G. A., "Direct Simulation Monte Carlo Method-Current Status and Prospects," and "The Formation and Reflection of Shock Waves," *Rarefied Gas Dynamics*, Supplement 5, Vol. I, Academic Press, New York, 1969, pp. 85–98 and 301–311.

[11] Vogenitz, F. W., Broadwell, J. E., and Bird, G. A., "Leading Edge Flow by the Monte Carlo Direct Simulation Technique," *AIAA Journal*, Vol. 8, No. 3, March 1970, pp. 504–510.

[12] McCroskey, W. J., Bogdonoff, S. M., and Genchi, A. P., *Rarefied Gas Dynamics*, Supplement 4, Vol. II, Academic Press, New York, 1967, pp. 1047.

[13] McCroskey, W. J., "Pressure Distributions on Sharp Cones in Rarefied Hypersonic Flow," *AIAA Journal*, Vol. 5, No. 11, Nov. 1967, pp. 2102–2104.

[14] Hickman, R. S., *Rarefied Gas Dynamics*, Supplement 4, Vol. II, Academic Press, New York, 1967.

[15] Waldron, H. F., "Viscous Hypersonic Flows Over Pointed Cones at Low Reynolds Numbers," Report 66-0111, June 1966 Aerospace Research Labs., Wright-Patterson Air Force Base, Ohio.

[16] Geiger, R. E., *Semi-Annual Report, DAH C04-67-C-0065*, Feb. 1968, G.E. Co., Valley Forge, Pa.

[17] Present, R. D., *Kinetic Theory of Gases*, McGraw-Hill, New York, 1958.

[18] Probstein, R. F., "Shock Wave and Flow Field Development in Hypersonic Reentry," *ARS Journal*, Feb. 1961, pp. 185–194.

[19] Hamel, B. B. and Cooper, A. L., "A First Collision Theory of the Hyperthermal Leading Edge Problem," *Rarefied Gas Dynamics*, Supplement 5, Vol. 1, Academic Press, New York, 1969, pp. 433–440.

[20] Metcalf, S. C., Lillicrap, D. C., and Berry, C. J., "A Study of the Effect of Surface Condition on the Shock Layer Development over Sharp Edged Shapes in Low Reynolds Number High Speed Flow," *Rarefied Gas Dynamics*, Supplement 5, Vol. I, Academic Press, New York, 1969, pp. 619–634.

[21] Bird, G. A., "The Structure of Rarefied Gas Flows Past Simple Aerodynamic Shapes," *Journal of Fluid Mechanics*, Vol. 36, Pt. 3, 1969, pp. 571–576.

[22] Laurmann, J. A., "First Collision Calculation of Cone Drag Under Hypersonic Rarefied Flow Conditions," *Astronautica Acta*, Vol. 13, 1967, pp. 401–404.

[23] Grad, H. and Hu, P. N., "Drag of a Slender Cone in Hypersonic Flow," *Rarefied Gas Dynamics*, Supplement 5, Vol. I, Academic Press, New York, 1969, pp. 561–573.

[24] Chapman, S. and Cowling, T. G., *The Mathematical Theory of Non-Uniform Gases*, Chap. 12, Cambridge University Press, 1960, p. 223.

[25] Schmidt, B., "Electron Beam Density Measurements in Shock Waves in Argon," *Journal of Fluid Mechanics*, Vol. 39, Pt. 2, 1969, pp. 361–373.

[26] Muckenfuss, C., "Mean Free Path Concept in Gas Dynamics," *The Physics of Fluids*, Vol. 5, No. 2, Feb. 1962, pp. 165–168.

[27] Ziering, S. and Ek, F., "Mean Free Path Definition in the Mott-Smith Shock Wave Solution," *The Physics of Fluids*, Vol. 4, No. 6, June 1961, pp. 765–766.

[28] Narasimha, R. and Deshpande, S. M., "Minimum Error Solutions of the Boltzmann Equation for Shock Structure," *Journal of Fluid Mechanics*, Vol. 36, Part 3, 1969, pp. 555–570.